Multiuser Cooperation with Hybrid Network Coding in Wireless Networks

Gengrun WANG, Daoxing GUO, Aijun LIU, Bangning ZHANG

Inst. of Communication Engineering, PLA University of Science and Technology,
Yudao Street, 2, 210007, Nanjing, China

wanggengrun@gmail.com, Dxguo1973@163.com, Ajliu1970@163.com, zhangbn@163.com

Abstract. *In this paper a hybrid Network Coding Cooperation (hybrid-NCC) system is proposed to achieve both reliable transmission and high throughput in wireless networks. To balance the transmission reliability with throughput, the users are divided into cooperative sub-networks based on the geographical information, and the cooperation is implemented in each sub-network. After receiving signals from the cooperative partners, each user encodes them by exploiting hybrid network coding and then forwards the recoded symbols via the Link-Adaptive Regenerative (LAR) relaying. First, the Diversity-Multiplexing Tradeoff (DMT) is analyzed to demonstrate that the proposed system is bandwidth-efficient. Second, the Symbol Error Probability (SEP) is also derived, which shows that the proposed system achieves a higher reliability as compared to the traditional Complex Field Network Coding Cooperation (CFNCC). Moreover, because dedicated relays are not required, our proposed system can both reduce the costs and enhance the flexibility of the implementation. Finally, the analytical results are supported and validated by numerical simulations.*

Keywords

Cooperative communication, complex field network coding, diversity-multiplexing tradeoff, wireless communication.

1. Introduction

In wireless networks, robust transmission against shadowing or enhanced coverage can be achieved from spatial diversity [1]. Typically, it is obtained by deploying multiple transmit and/or multiple receive antennas at base stations and/or mobile ends, such as found in Multi-Input Multi-Out (MIMO) systems. However, collocated antennas necessary for MIMO systems are not practical for mobile ends, due to their size and power limitations. In order to acquire the spatial diversity from these functionally limited hand-held mobile ends, cooperative communication has attracted much research interest. In cooperative communication, a virtual MIMO system is established through cooperation among multiple mobile ends. The cooperative ends in this system transmit signals for both themselves and their partners.

Although the cooperative system is robust, it is at the expense of other performance such as throughput. In order to avoid interference, transmissions should be in orthogonal channels. Therefore, the throughput decreases when the cooperative network size is large. Given this, a tradeoff must be made between the transmission reliability and the throughput.

Network coding is believed to be able to improve the throughput of the traditional communication strategies [2]. Therefore, incorporating network coding into the cooperative communication has been an attractive topic. Chen et al. have analyzed the achieved diversity of a wireless communication system adopting network coding [3]. Katti et al. have combined the Galois Field Network Coding (GFNC) theory with practical applications [4]. A system in which the relay implemented the Analog Network Coding (ANC) to assist the transmission was proposed, which reduced the system complexity and achieved the same Diversity-Multiplexing Tradeoff (DMT) as the GFNC strategy did under certain conditions [5]. Peng et al. have proposed a mechanism which achieved good DMT performance by adopting the network coding dynamically [6]. Complex Field Network Coding (CFNC) applied to the cooperative network was introduced by Wang et al. [7], and has been studied by other researchers [8], [9]. The remarkable characteristic of CFNC Cooperation (CFNCC) is the desirable throughput. However, the lower coding gains limit the application of the CFNC strategy in large scale networks.

In this paper a hybrid Network Coding Cooperation (hybrid-NCC) system suitable for multiuser wireless networks is proposed. Taking advantage of both GFNC and CFNC, the hybrid-NCC is implemented in divisional cooperative sub-networks, and acquires robust transmission along with high throughput. The DMT and the Symbol Error Probability (SEP) of this system are analyzed. It is proved that the proposed hybrid-NCC system has achieved desirable DMT performance, and at the same time full diversity is obtained. The SEP of the system is effectively

decreased compared with CFNCC [7], although the spectral efficiency is slightly reduced. Therefore, the transmission reliability is improved. Additionally, the deployment of dedicated relay stations is not required, which reduces the costs of the implementation.

The remainder of the paper is organized as follows. In Section 2, the transmission procedure of the hybrid-NCC system is presented in detail. The DMT performance is analyzed in Section 3, and the SEP performance is deduced in the following section. Simulation tests are shown in Section 5. At last, conclusions are drawn in Section 6.

2. Proposed Scheme and System Model

In a multiuser wireless network, users can be divided into cooperative sub-networks by the grouping and partner selection protocol [10]. A cooperative sub-network may consist of N users and one base station, represented as (N, 1). This sub-network is a basic portion of the multiuser system and an essential scenario to be analyzed. For simplicity, we take $N = 3$ as an example.

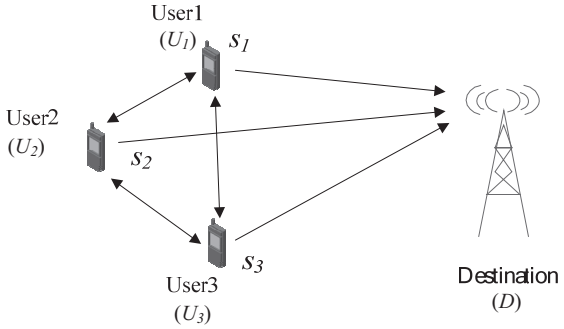

Fig. 1. A cooperative sub-network with three users and one base station.

This (3, 1) setup model is shown in Fig. 1. The transmit information of user i (U_i) is denoted by s_i. In this system, every user is the relay of the other cooperative users in its idle state. Users decode the information sent by their partners, encode them by hybrid Network Coding (hybrid-NC) proposed in this paper and then forward the encoded signals to the common destination (D).

In this paper the channels are block Rayleigh fading. The fading coefficient of the channel between U_j and U_i is denoted by h_{ij}. It represents the effects of path-loss, shadowing and frequency non-selective fading, and is modeled as a zero-mean, independent, circularly symmetric complex Gaussian random variable with a variance of δ_{ij}^2. The fading coefficients keep constant during one period, and vary over different periods. The noise effect and other forms of interference are represented by n_{ij}. It is modeled as a zero-mean mutually independent, circularly symmetric, complex Gaussian random sequence with a variance of N_0. The instantaneous and average received Signal-to-Noise Ratio (SNR) are given respectively by $\gamma_{ij} = |h_{ij}|^2\gamma_0$ and $\bar{\gamma}_{ij} = \delta_{ij}^2\gamma_0$, where $\gamma_0 = P_x/N_0$ denotes the SNR without fading and P_x is the average transmit power. We assume that the channel state information is accurately measured at the appropriate receivers via training symbols sent by the transmit terminals, but not fully known by the transmitters.

Considering of current limitations in radio implementation, the users' antennas are half-duplex. The transmission procedure is divided into several orthogonal sub-channels, and non-overlapping time slots are allocated to different users. The time-division channel allocation for this model is illustrated in Fig. 2. In this figure, the transmission procedure is divided into two phases. The first three time slots compose the Direct Transmission Phase (DTP), and the last time slot is the Hybrid Network Coding and Forwarding Phase (HNCFP). During the DTP, every user transmits its signal in the separated time slot, and receives signals from its partners in the other two time slots. During the HNCFP, users encode the information from their partners by the hybrid-NC, and then transmit the encoded signals simultaneously to the base station by the Link-Adaptive Regenerative (LAR) forwarding strategy of [11]. In every block, D receives separated signals from the users in the DTP and the hybrid-NC coded signals in the HNCFP.

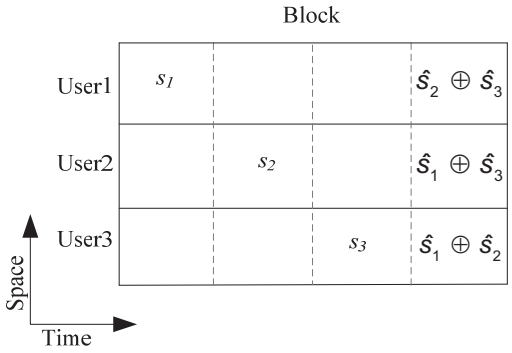

Fig. 2. The time-division structure for the proposed hybrid-NCC system.

As shown in Fig. 2, each user does not transmit signals over the whole block; it only utilizes one separated time slot to transmit its signal, and the last time slot to transmit the coded signals of its partners. For simplicity, we take U_1 as an example.

In the first time slot of DTP, U_1 broadcasts its signal to U_2, U_3 and D. The signals received by the partners and D are expressed as follows:

$$y_{21} = h_{21}s_1 + n_{21}, \tag{1}$$

$$y_{31} = h_{31}s_1 + n_{31}, \tag{2}$$

$$y_{1d} = h_{1d}^D s_1 + n_{1d} \tag{3}$$

where s_1 represents the signal sent by U_1 and is drawn from a finite alphabet A_s, γ_{ij} represents the signal of U_j received by U_i, γ_{1d} represents the signal received by D during DTP, h_{id}^D is the fading coefficient of the channel between U_i and D during DTP.

$$(\hat{s}_1,\hat{s}_2,\hat{s}_3)=\arg\min_{s_1,s_2,s_3\in \mathrm{A}_s}\left\{\left\|y_{1d}-h_{1d}^{D}s_1\right\|^2+\left\|y_{2d}-h_{2d}^{D}s_2\right\|^2+\left\|y_{3d}-h_{3d}^{D}s_3\right\|^2 +\left\|y_{4d}-\left[h_{1d}^{R}\sqrt{\alpha_1}\theta_1(s_2\oplus s_3)+h_{2d}^{R}\sqrt{\alpha_2}\theta_2(s_1\oplus s_3)+h_{3d}^{R}\sqrt{\alpha_3}\theta_3(s_1\oplus s_2)\right]\right\|^2\right\} \tag{13}$$

Similarly, in the second and the third time slots, U_2 and U_3 broadcast signals separately. The signals received by U_1 and D are given by:

$$y_{12}=h_{12}s_2+n_{12}\ , \tag{4}$$

$$y_{13}=h_{13}s_3+n_{13}\ , \tag{5}$$

$$y_{2d}=h_{2d}^{D}s_2+n_{2d}\ , \tag{6}$$

$$y_{3d}=h_{3d}^{D}s_3+n_{3d}\ . \tag{7}$$

Then, U_1 attempts to retrieve information from the received signals by the Maximum Likelihood (ML) demodulation. The estimated signals are:

$$\hat{s}_2=\arg\min_{s\in \mathrm{A}_s}\left\|y_{12}-h_{12}s\right\|^2, \tag{8}$$

$$\hat{s}_3=\arg\min_{s\in \mathrm{A}_s}\left\|y_{13}-h_{13}s\right\|^2. \tag{9}$$

During the HNCFP, U_1 recodes the retrieved signals, initially by GFNC (i.e. XOR operation), and obtains:

$$x_1=\hat{s}_2\oplus\hat{s}_3\ . \tag{10}$$

Next, U_1 encodes x_1 by CFNC and then sends the recoded signal to D simultaneously with its partners by the LAR strategy.

The signal received by D during this phase is:

$$y_{4d}=\sum_{i=1}^{3}h_{id}^{R}\sqrt{\alpha_i}\theta_i x_i+n_{4d} \tag{11}$$

where y_{4d} denotes the signal received by D during HNCFP, h_{id}^{R} is the channel fading coefficient in this phase, and the superscript R indicates that U_i works as a relay of its partners, α_i represents the link-adaptive scalar and controls the transmit power at U_i during HNCFP, θ_i is drawn from the complex field X. The design of θ_i is studied in the references [12], [13], which considered the choice of θ_i based on the linear constellation precoding of MIMO systems. We adopt this design and rewrite the rules here:

$$\theta_{i,i=1,\ldots,N}=\begin{cases}\exp\left[j\pi(4n-1)(i-1)/2N\right], & \text{for } N=2^k\\ \exp\left[j\pi(6n-1)(i-1)/3N\right], & \text{for } N=3\times 2^k\end{cases} \tag{12}$$

for any $n=1,\cdots,N$.

One of the distinct features of CFNC is the one-to-one mapping between the ordered pair $[x_1,x_2,x_3]^T$ and $y=\theta_1x_1+\theta_2x_2+\theta_3x_3$, which means that if and only if $[x_1^i,x_2^i,x_3^i]^T=[x_1^j,x_2^j,x_3^j]^T$, $y_i=y_j$. This feature enables the receiver detects $[x_1,x_2,x_3]^T$ based only on the received symbol y.

Given that $h_{id}^{R}\sqrt{\alpha_i}$ is obtained at D through channel training, and $\boldsymbol{\theta}:=[\theta_1,\theta_2,\theta_3]^T$ is known by all of the users and D, the ML detector at D can be expressed as shown in (13) at the top of the page.

3. DMT Performance

In this section, the DMT performance of the proposed system is analyzed. This performance indicates the relationship between the information rate and the reliability of the transmission [14].

The DMT is described as:

$$DMT=-\lim_{\gamma\to\infty}\frac{\log_2 P_{out}\left(r\log_2\gamma\right)}{\log_2\gamma}. \tag{14}$$

In this equation, the diversity gain is:

$$d=-\lim_{\gamma\to\infty}\frac{\log_2 P_{out}\left(R,\gamma\right)}{\log_2\gamma} \tag{15}$$

and the multiplexing gain is:

$$r=-\lim_{\gamma\to\infty}\frac{R(\gamma)}{\log_2\gamma} \tag{16}$$

where P_{out} is the outage probability of the transmission with the received SNR γ. The data rate R at the given multiplexing gain r is

$$R=r\log_2(1+\gamma)\ . \tag{17}$$

Without loss of generality, we take U_1 as an example. The outage probability for U_1 - D is calculated as:

$$P_{out}=P_{C1}\cdot P_{FC}+P_{C2}\cdot P_{PC2}+P_{C3}\cdot P_{PC3}+P_{C4}\cdot P_{NC} \tag{18}$$

where P_{C1} denotes the probability of the case that both of the following requirements are met:

a) During the DTP, no outage occurs in the U_1-U_2 and U_2-U_3 link pairs, then U_2 transmits the correct symbol $x_2=s_1\oplus s_3$ to D; and at the same time no outage occurs in the U_3 - D link pair. Then D will retrieve s_1 by $\hat{x}_2\oplus\hat{s}_3$ using the correct symbol s_3.

b) Similarly, there is no outage occurrence in the U_1-U_3, U_2-U_3 and U_2-D link pairs during the DTP. Therefore, D will retrieve s_1 by $\hat{x}_3\oplus\hat{s}_2$ using the correct symbol s_2.

The outage probability in this case is denoted as P_{FC}. P_{PC2} is the outage probability of the partial cooperation in the

case that requirement (a) is satisfied but (b) is not; and the occurrence probability of this partial cooperation is denoted as P_{C2}. P_{PC3} is defined similarly to P_{PC2}, in the case that requirement (b) is satisfied but (a) is not; and the occurrence probability is denoted as P_{C3}. The occurrence probability for the case that neither (a) nor (b) is satisfied, is denoted as P_{C4}; and in this case, the outage probability is P_{NC}.

First, we deduce the conditional probability P_{C1}. In this case, U_2 receives signals from U_1 and U_3 during DTP without the occurrence of outage. Besides, D correctly retrieves the signal of U_3 in order to decode x_2 sent by U_2 during the HNCFP. Meanwhile, U_3 works in the same way as described above. Then the probability P_{C1} can be expressed as:

$$\begin{aligned} P_{C1} &= P_a \cdot P_b \\ &= [(1-P_{out}^{21})\cdot(1-P_{out}^{23})\cdot(1-P_{out}^{3d})]\cdot[(1-P_{out}^{31})\cdot(1-P_{out}^{32})\cdot(1-P_{out}^{2d})] \\ &= \{[1-P(I_{21}<R_1)]\cdot[1-P(I_{23}<R_3)]\cdot[1-P(I_{3d}<R_3)]\} \\ &\cdot\{[1-P(I_{31}<R_1)]\cdot[1-P(I_{32}<R_2)]\cdot[1-P(I_{2d}<R_2)]\} \end{aligned} \tag{19}$$

where P_a denotes the occurrence probability of (a), P_b denotes the occurrence probability of (b), and P_{out}^{ji} is the outage probability of the link U_i - U_j. With coherent detection, the mutual information of U_i - U_j is given by:

$$I_{ji} = \frac{3}{4}\log_2(1+|h_{ji}|^2\,\gamma_0) \tag{20}$$

where the mutual information is divided by 4/3, because four time slots are assigned to three U - D pairs. Similarly, the mutual information of U_i -D is given by:

$$I_{id} = \frac{3}{4}\log_2(1+|h_{id}^D|^2\,\gamma_0)\,. \tag{21}$$

Then, the outage probability of U_1 - U_2 with the transmit power P_x and rate R_1, is given by:

$$\begin{aligned} P_{out}^{21} &= P(I_{21}<R_1) = P\{\frac{3}{4}\log_2(1+|h_{21}|^2\,\gamma_0)<R_1\} \\ &= 1-\exp(-\frac{2^{\frac{4}{3}R_1}-1}{\delta_{21}^2\gamma_0}) \end{aligned} \tag{22}$$

The other outage probabilities in (19) are calculated similarly. By substituting them into (19), the occurrence probability P_{C1} is obtained as:

$$\begin{aligned} P_{C1} &= \exp(-\frac{2^{\frac{4}{3}R_1}-1}{\delta_{21}^2\gamma_0})\cdot\exp(-\frac{2^{\frac{4}{3}R_3}-1}{\delta_{23}^2\gamma_0})\cdot\exp(-\frac{2^{\frac{4}{3}R_3}-1}{\delta_{3d}^2\gamma_0}) \\ &\cdot\exp(-\frac{2^{\frac{4}{3}R_1}-1}{\delta_{31}^2\gamma_0})\cdot\exp(-\frac{2^{\frac{4}{3}R_2}-1}{\delta_{32}^2\gamma_0})\cdot\exp(-\frac{2^{\frac{4}{3}R_2}-1}{\delta_{2d}^2\gamma_0}) \end{aligned} \tag{23}$$

In the similar manner, the occurrence probabilities P_{C2}, P_{C3} and P_{C4} are:

$$\begin{aligned} P_{C2} &= \exp(-\frac{2^{\frac{4}{3}R_1}-1}{\delta_{21}^2\gamma_0})\cdot\exp(-\frac{2^{\frac{4}{3}R_3}-1}{\delta_{23}^2\gamma_0})\cdot\exp(-\frac{2^{\frac{4}{3}R_3}-1}{\delta_{3d}^2\gamma_0}) \\ &\cdot\left[1-\exp(-\frac{2^{\frac{4}{3}R_1}-1}{\delta_{31}^2\gamma_0})\cdot\exp(-\frac{2^{\frac{4}{3}R_2}-1}{\delta_{32}^2\gamma_0})\cdot\exp(-\frac{2^{\frac{4}{3}R_2}-1}{\delta_{2d}^2\gamma_0})\right] \end{aligned} \tag{24}$$

$$\begin{aligned} P_{C3} &= \left[1-\exp(-\frac{2^{\frac{4}{3}R_1}-1}{\delta_{21}^2\gamma_0})\cdot\exp(-\frac{2^{\frac{4}{3}R_3}-1}{\delta_{23}^2\gamma_0})\cdot\exp(-\frac{2^{\frac{4}{3}R_3}-1}{\delta_{3d}^2\gamma_0})\right] \\ &\cdot\exp(-\frac{2^{\frac{4}{3}R_1}-1}{\delta_{31}^2\gamma_0})\cdot\exp(-\frac{2^{\frac{4}{3}R_2}-1}{\delta_{32}^2\gamma_0})\cdot\exp(-\frac{2^{\frac{4}{3}R_2}-1}{\delta_{2d}^2\gamma_0}) \end{aligned} \tag{25}$$

$$\begin{aligned} P_{C4} &= \left[1-\exp(-\frac{2^{\frac{4}{3}R_1}-1}{\delta_{21}^2\gamma_0})\cdot\exp(-\frac{2^{\frac{4}{3}R_3}-1}{\delta_{23}^2\gamma_0})\cdot\exp(-\frac{2^{\frac{4}{3}R_3}-1}{\delta_{3d}^2\gamma_0})\right] \\ &\cdot\left[1-\exp(-\frac{2^{\frac{4}{3}R_1}-1}{\delta_{31}^2\gamma_0})\cdot\exp(-\frac{2^{\frac{4}{3}R_2}-1}{\delta_{32}^2\gamma_0})\cdot\exp(-\frac{2^{\frac{4}{3}R_2}-1}{\delta_{2d}^2\gamma_0})\right] \end{aligned} \tag{26}$$

In the following part, we analyze the outage probabilities in these cases. For simplicity, we consider the case of identical symbol rate for all users, i.e. $R_1 = R_2 = R_3$.

First of all, we propose three equivalent one-transmitter, one-receiver links during the HNCFP. This proposition means that each user will *separately* provide an equivalent copy of information, received during the DTP, to D. Without loss of generality, we take the link U_2 - D during the HNCFP, for the example.

Let $d^{\min}$ ($d^{\max}$) denotes the minimum (maximum) Euclidean distance in the constellation of x_2, and $d_{r_2d}^{\min}$ ($d_{r_2d}^{\max}$) denotes the minimum (maximum) Euclidean distance of symbols, which are encoded by different x_2, in the constellation of $\boldsymbol{\theta}^T\mathbf{H}_{sd}^R\mathbf{x}$, where $\mathbf{H}_{sd}^R := diag(h_{1d}^R, h_{2d}^R, h_{3d}^R)$, $\mathbf{x} := [x_1, x_2, x_3]^T$. Then, we build a *virtual* U_2 - D link during HNCFP without power scaling, and the I/O relationship is:

$$\tilde{y}_{r_2d} = \tilde{h}_{2d}^R x_2 + \tilde{n}_{4d} \tag{27}$$

where $\tilde{h}_{2d}^R$ has an arbitrary phase known by D, with an amplitude $|\tilde{h}_{2d}^R| := d_{r_2d}^{\min}/d^{\max}$. Then, the maximum Euclidean distance of the received constellation in (27) is $|\tilde{h}_{2d}^R|\,d^{\max}\sqrt{P_x} = d_{r_2d}^{\min}$, which equals the minimum Euclidean distance of symbols encoded by different x_2, in the constellation of $\boldsymbol{\theta}^T\mathbf{H}_{sd}^R\mathbf{x}$. Therefore, the instantaneous received SNR of this *virtual* link, namely $\tilde{\gamma}_{r_2d} = |\tilde{h}_{2d}^R|^2\,\gamma_0$, is the lower SNR bound of the original U_2 - D link during the HNCFP.

Similarly, we define the I/O relationship:

$$\tilde{y}_{4d} = \tilde{h}_{rd}\boldsymbol{\theta}^T\mathbf{x} + \tilde{n}_{4d} = \tilde{h}_{rd}u + \tilde{n}_{4d} \tag{28}$$

where $u := \boldsymbol{\theta}^T\mathbf{x}$, $\tilde{h}_{rd}$ is defined in the same way as the definition of $\tilde{h}_{2d}^R$, by replacing x_2 with u. $\tilde{\gamma}_{rd}$ is the instantaneous received SNR of this *virtual* link, and then it is obvious that $\tilde{\gamma}_{rd} \le \tilde{\gamma}_{r_2d}$. Due to lemma 1 in [7]:

$$\Delta_{rd}\gamma_{rd}^{\min} \le \tilde{\gamma}_{rd} \tag{29}$$

where Δ_{rd} is a random variable independent of $\gamma_{rd}^{\min}$ satisfying $P(\Delta_{rd} > 0) = 1$, $\gamma_{rd}^{\min}$ is the minimum received SNR of the actual links, which is defined as $\gamma_{rd}^{\min} := \min(\gamma_{r_1d}, \gamma_{r_2d}, \gamma_{r_3d})$, where $\gamma_{r_id} := |h_{id}^R|^2\,\gamma_0, \forall i = 1,2,3$. Furthermore, $\gamma_{rd}^{\min}$ is exponentially distributed with the parameter δ_{rd}^2, where $\delta_{rd}^2 = 1/\sum_{i=1}^{3}(1/\delta_{r_id}^2)$ [6].

Then, $\tilde{\gamma}_{r_2d}$ can be further bounded by $\gamma_{rd}^{\min}$:

$$\tilde{\gamma}_{r_2d} \ge \Delta_{rd}\gamma_{rd}^{\min}. \tag{30}$$

The instantaneous lower SNR bound of the *virtual* link U_3 - D (i.e. $\tilde{\gamma}_{r_3d}$) during the HNCFP can also be analogously defined.

Next, we calculate the outage probability P_{FC}.

First, the lower bound of mutual information for $U_1 - D$ over the whole block in this case is:

$$I_{1d}^B \ge \frac{3}{4}\log_2(1 + \gamma_{1d}^D + \alpha_2\tilde{\gamma}_{r_2d} + \alpha_3\tilde{\gamma}_{r_3d}). \tag{31}$$

Second, the upper bound of the outage probability P_{FC} is obtained as:

$$\begin{aligned} P_{\mathrm{FC}} &= P(I_{1d}^B < R_1) \\ &\le P\left\{\frac{3}{4}\log_2(1 + \gamma_{1d}^D + \alpha_2\tilde{\gamma}_{r_2d} + \alpha_3\tilde{\gamma}_{r_3d}) < R_1\right\} \end{aligned} \tag{32}$$

Then, the upper bound of (32) is obtained as shown in (33) at the bottom of the page, where:

$$\Delta := (2^{4R_1/3} - 1)/\gamma_0, V_1 := \delta_{1d}^2, V_2 := \alpha_2\Delta_{rd}\delta_{rd}^2, V_3 := \alpha_3\Delta_{rd}\delta_{rd}^2.$$

In the same way, the upper bounds of outage probabilities for the other three cases are obtained as:

$$\begin{aligned} P_{\mathrm{PC2}} &\le P\{\frac{3}{4}\log_2(1 + |h_{1d}|^2\gamma_0 + \alpha_2|\tilde{h}_{2d}^R|^2\gamma_0) < R_1\} \\ &= P[|h_{1d}|^2 + \alpha_2|\tilde{h}_{2d}^R|^2 < \Delta] \\ &\le \begin{cases} 1 - [1 + \frac{\Delta}{V_1}] \times \exp(-\frac{\Delta}{V_1}), & V_1 = V_2 \\ 1 - \frac{V_1\exp(-\frac{\Delta}{V_1})}{V_1 - V_2} - \frac{V_2\exp(-\frac{\Delta}{V_2})}{V_2 - V_1}, & V_1 \ne V_2 \end{cases} \end{aligned} \tag{34}$$

$$\begin{aligned} P_{\mathrm{PC3}} &\le P\{\frac{3}{4}\log_2(1 + |h_{1d}|^2\gamma_0 + \alpha_3|\tilde{h}_{3d}^R|^2\gamma_0) < R_1\} \\ &= P[|h_{1d}|^2 + \alpha_3|\tilde{h}_{3d}^R|^2 < \Delta] \\ &\le \begin{cases} 1 - [1 + \frac{\Delta}{V_1}] \times \exp(-\frac{\Delta}{V_1}), & V_1 = V_3 \\ 1 - \frac{V_1\exp(-\frac{\Delta}{V_1})}{V_1 - V_3} - \frac{V_3\exp(-\frac{\Delta}{V_3})}{V_3 - V_1}, & V_1 \ne V_3 \end{cases} \end{aligned} \tag{35}$$

$$\begin{aligned} P_{NC} &= P(I_{1d} < R_1) = P\left\{\frac{3}{4}\log_2(1 + |h_{1d}|^2\gamma_0) < R_1\right\} \\ &= 1 - \exp(-\frac{\Delta}{V_1}) \end{aligned} \tag{36}$$

By substituting (23)-(26) and (33)-(36) into (18), an upper bound of the outage probability for U_1 - D is obtained. In what follows, we present the DMT of the proposed scheme on the basis of the analysis above.

When $\gamma_0 \to \infty$, the outage probability U_1 - D will be expressed as detailed below:

$$\begin{aligned} \lim_{\gamma_0\to\infty} P_{out}(\gamma_0) = &\lim_{\gamma_0\to\infty} P_{C1}\cdot P_{FC} + \lim_{\gamma_0\to\infty} P_{C2}\cdot P_{PC2} \\ &+ \lim_{\gamma_0\to\infty} P_{C3}\cdot P_{PC3} + \lim_{\gamma_0\to\infty} P_{C4}\cdot P_{NC}. \end{aligned} \tag{37}$$

Due to (23)-(26), terms in the right-hand side of (37) are:

$$P_{\mathrm{FC}} \le P\left\{\frac{3}{4}\log_2(1 + \gamma_{1d}^D + \alpha_2\tilde{\gamma}_{r_2d} + \alpha_3\tilde{\gamma}_{r_3d}) < R_1\right\} = P\left[|h_{1d}|^2 + \alpha_2|\tilde{h}_{2d}^R|^2 + \alpha_3|\tilde{h}_{3d}^R|^2 < \Delta\right]$$

$$\le \begin{cases} 1 - [1 + \frac{\Delta}{V_1} + \frac{1}{2}\times(\frac{\Delta}{V_1})^2] \times \exp(-\frac{\Delta}{V_1}) & V_1 = V_2 = V_3 \\ 1 + \frac{(V_1 - V_2)\cdot\Delta + 2V_1\cdot V_2}{(V_1 - V_2)^2}\cdot\exp(-\frac{\Delta}{V_2}) - \sum_{i=1}^{2}\frac{V_i^2\exp(-\frac{\Delta}{V_i})}{(V_1 - V_2)^2} & V_1 \ne V_2, V_2 = V_3 \\ 1 - \sum\limits_{\substack{i=1 \\ j,k\in\{1,2,3\} \\ j\ne i, k\ne i, j\ne k}}^{3}\frac{V_i^2\exp(-\frac{\Delta}{V_i})}{(V_i - V_j)\cdot(V_i - V_k)} & V_1 \ne V_2, V_1 \ne V_3, V_2 \ne V_3 \end{cases} \tag{33}$$

$$\lim_{\gamma_0\to\infty} P_{C1} = 1, \tag{38}$$

$$\lim_{\gamma_0\to\infty} P_{C2} = \lim_{\gamma_0\to\infty}\left[1-\exp\left(-\frac{\Delta}{\delta_{31}^2}\right)\cdot\exp\left(-\frac{\Delta}{\delta_{32}^2}\right)\exp\left(-\frac{\Delta}{\delta_{2d}^2}\right)\right] = \frac{\Delta}{\delta_{31}^2}+\frac{\Delta}{\delta_{32}^2}+\frac{\Delta}{\delta_{2d}^2}+\mathrm{O}\left(\frac{1}{\gamma_0}\right), \tag{39}$$

$$\lim_{\gamma_0\to\infty} P_{C3} = \lim_{\gamma_0\to\infty}\left[1-\exp\left(-\frac{\Delta}{\delta_{21}^2}\right)\cdot\exp\left(-\frac{\Delta}{\delta_{23}^2}\right)\exp\left(-\frac{\Delta}{\delta_{3d}^2}\right)\right] = \frac{\Delta}{\delta_{21}^2}+\frac{\Delta}{\delta_{23}^2}+\frac{\Delta}{\delta_{3d}^2}+\mathrm{O}\left(\frac{1}{\gamma_0}\right), \tag{40}$$

$$\lim_{\gamma_0\to\infty} P_{C4} = \lim_{\gamma_0\to\infty}\left\{\left[1-\exp\left(-\frac{\Delta}{\delta_{31}^2}\right)\cdot\exp\left(-\frac{\Delta}{\delta_{32}^2}\right)\exp\left(-\frac{\Delta}{\delta_{2d}^2}\right)\right]\cdot\left[1-\exp\left(-\frac{\Delta}{\delta_{21}^2}\right)\cdot\exp\left(-\frac{\Delta}{\delta_{23}^2}\right)\exp\left(-\frac{\Delta}{\delta_{3d}^2}\right)\right]\right\} = \left(\frac{\Delta}{\delta_{31}^2}+\frac{\Delta}{\delta_{32}^2}+\frac{\Delta}{\delta_{2d}^2}\right)\cdot\left(\frac{\Delta}{\delta_{21}^2}+\frac{\Delta}{\delta_{23}^2}+\frac{\Delta}{\delta_{3d}^2}\right)+\mathrm{O}\left(\frac{1}{\gamma_0^2}\right), \tag{41}$$

where $\mathrm{O}(\cdot)$ represents the higher-order terms.

Additionally, the upper bound of P_{FC} with $\gamma_0\to\infty$ can be derived from (33) and shown as:

$$\lim_{\gamma_0\to\infty} P_{FC} \le \lim_{\gamma_0\to\infty} P\left\{\frac{3}{4}\log_2(1+\gamma_{1d}^R+\alpha_2\tilde{\gamma}_{r_2d}+\alpha_3\tilde{\gamma}_{r_3d})<R_1\right\} \le \begin{cases} \frac{\Delta^3}{6}\left[\frac{1}{V_1\cdot(V_1-V_2)\cdot(V_1-V_3)}+\frac{1}{V_2\cdot(V_2-V_1)\cdot(V_2-V_3)}\right. \\ \left.+\frac{1}{V_3\cdot(V_3-V_2)\cdot(V_3-V_1)}\right]+\mathrm{O}(\frac{1}{\gamma_0^3}) & V_1\neq V_2, V_1\neq V_3, V_2\neq V_3 \\ \frac{\Delta^3}{6V_1\cdot V_2\cdot V_3}+\mathrm{O}(\frac{1}{\gamma_0^3}) & else \end{cases} \tag{42}$$

By adopting the result of Appendix A from [15], the outage probabilities for the partial cooperation cases are:

$$\lim_{\gamma_0\to\infty} P_{PC2} \le \lim_{\gamma_0\to\infty} P\left\{\frac{3}{4}\log_2(1+\gamma_{1d}^R+\alpha_2\tilde{\gamma}_{r_2d})<R_1\right\} \le \frac{2}{V_1\cdot V_2}\cdot\Delta^2+\mathrm{O}(\frac{1}{\gamma_0^2}) \tag{43}$$

$$\lim_{\gamma_0\to\infty} P_{PC3} \le \lim_{\gamma_0\to\infty} P\left\{\frac{3}{4}\log_2(1+\gamma_{1d}^R+\alpha_3\tilde{\gamma}_{r_3d})<R_1\right\} \le \frac{2}{V_1\cdot V_3}\cdot\Delta^2+\mathrm{O}(\frac{1}{\gamma_0^2}) \tag{44}$$

In addition, P_{NC} with $\gamma_0\to\infty$ will be:

$$\lim_{\gamma_0\to\infty} P_{NC} = \lim_{\gamma_0\to\infty}[1-\exp(-\frac{\Delta}{V_1})] = \frac{\Delta}{V_1}+\mathrm{O}(\frac{1}{\gamma_0}). \tag{45}$$

By replacing the data rate of U_1 (R_1) with the multiplexing gain (r_1), i.e. $R_1 = r_1\log(\gamma_0)$, and then substituting (38)-(45) into (37), the DMT (14) of the proposed system is:

$$d(r_1) = 3\times(1-\frac{4}{3}r_1). \tag{46}$$

In the case of a three-user cooperative network, (3, 1) for the proposed system and (3, 1, 1) for other scenarios with a relay, we compare the DMT performance. It showed that Conventional Cooperation (CC) systems, such as Space-Time Coded Cooperation (STCC) and Opportunistic Relaying (OR), achieved the DMT of $d(r)=2\cdot(1-2r)$ [16,] [17]. The Network Coding Cooperation with Dynamic Coding (DC-NCC) achieved the DMT of $d(r)=2\cdot(1-4r/3)$ [6]. Additionally, the DMT of the CFNCC was $d(r)=2\cdot(1-r)$ [7]. The DMTs for different systems are illustrated in Fig. 3. It demonstrates that compared with the CC and DC-NCC, the hybrid-NCC achieves more diversity gains with the same expense of spectral efficiency, or with higher spectral efficiency for the same diversity gains. While compared with the CFNCC, it can be inferred that the Hybrid-NCC achieves the higher diversity gains at the cost of the spectral efficiency.

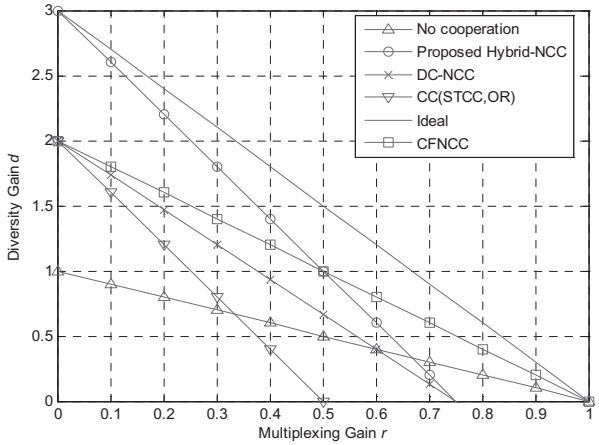

Fig. 3. The DMTs for different systems at the same symbol rate of users.

4. SEP Performance

In this section, the SEP performance of the proposed system is analyzed, where the SEP denotes the error probability of the user's symbols at D. Similarly, we take U_1 for an example.

During the DTP, the SEP of the link U_i- U_j or U_i- D ($\forall i,j\in\{1,2,3\}$) is:

$$P_{ji}^e = (M-1)Q\sqrt{2\gamma_{ji}} \le (M-1)\cdot\exp(-\gamma_{ji}) \tag{47}$$

where $M := |A_s|$, $Q(x) := (1/\sqrt{2\pi})\int_0^\infty \exp(-t^2/2)dt$. The last inequality follows from the Chernoff bound.

$$P_s = P_1 \cdot P_{FC} + P_3 \cdot P_{PC2} + P_4 \cdot P_{PC3} + P_2 \cdot P_{NC} \le P_{FC} + (1-P_{r_3}) \cdot P_{PC2} + (1-P_{r_2}) \cdot P_{PC3} + (1-P_{r_2}) \cdot (1-P_{r_3}) \cdot P_{NC}$$
$$\le (M-1) \cdot Q[\sqrt{2(\gamma_{1d} + \alpha_2 \tilde{\gamma}_{r_2 d} + \alpha_3 \tilde{\gamma}_{r_3 d})}] + (M-1)^2 [\exp(-\gamma_{31}) + \exp(-\gamma_{32}) + \exp(-\gamma_{2d}^D)] \cdot Q\left[\frac{\sqrt{2}\left(\gamma_{1d} + \alpha_2 \tilde{\gamma}_{r_2 d} - 2\alpha_3 \tilde{\gamma}_{r_3 d}\beta\right)}{\sqrt{\gamma_{1d} + \alpha_2 \tilde{\gamma}_{r_2 d} + 2\alpha_3 \tilde{\gamma}_{r_3 d}\beta}}\right]$$
$$+ (M-1)^2 [\exp(-\gamma_{21}) + \exp(-\gamma_{23}) + \exp(-\gamma_{3d}^D)] \cdot Q\left[\frac{\sqrt{2}\left(\gamma_{1d} - 2\alpha_2 \tilde{\gamma}_{r_2 d}\beta + \alpha_3 \tilde{\gamma}_{r_3 d}\right)}{\sqrt{\gamma_{1d} + 2\alpha_2 \tilde{\gamma}_{r_2 d}\beta + \alpha_3 \tilde{\gamma}_{r_3 d}}}\right]$$
$$+ (M-1)^3 [\exp(-\gamma_{21}) + \exp(-\gamma_{23}) + \exp(-\gamma_{3d}^D)] \cdot [\exp(-\gamma_{31}) + \exp(-\gamma_{32}) + \exp(-\gamma_{2d}^D)] \cdot Q\left[\frac{\sqrt{2}\left(\gamma_{1d} - 2\alpha_2 \tilde{\gamma}_{r_2 d}\beta - 2\alpha_3 \tilde{\gamma}_{r_3 d}\beta\right)}{\sqrt{\gamma_{1d} + 2\alpha_2 \tilde{\gamma}_{r_2 d}\beta + 2\alpha_3 \tilde{\gamma}_{r_3 d}\beta}}\right] \quad (58)$$

During the HNCFP, the ML detector at D, utilizing information from the whole block, is equivalent to the Maximum Ratio Combining (MRC).

In the proposed system, α_i is chosen to control the transmit power at U_i during the HNCFP, and it critically affects the SEP. By adopting the one introduced by Wang et al. [11], a diversity-achieving α for the relay (e.g. U_2) is:

$$\alpha_2 = \frac{\min(\gamma_{R_2}, \overline{\gamma}_{r_2 d})}{\overline{\gamma}_{r_2 d}} \quad (48)$$

where $\gamma_{R_2} \coloneqq \min\{\gamma_{21}, \gamma_{23}, \overline{\gamma}_{3d}\}$, $\overline{\gamma}_{r_2 d}$ is the equivalent average SNR of the *virtual* U_2 - D link during the HNCFP. $\overline{\gamma}_{3d}$ and $\overline{\gamma}_{r_2 d}$ are easily estimated infrequently by D, and the overhead of feeding back the statistical data to U_2 is then affordable. When links during the DTP are unreliable, then α_2 will be set as a small number, and when these links are reliable, it will be set as a large number.

Next, the SEPs for the different cases are analyzed, according to the cooperation types of U_1's partners.

First, we suppose that U_2 obtains signals from U_1 and U_3 correctly, and the signal of U_3 is also obtained correctly by D, during the DTP. Then, U_2 can provide a correct copy of U_1's information to D. The occurrence probability of this case is:

$$P_{r_2} = (1-P_{21}^e) \cdot (1-P_{23}^e) \cdot (1-P_{3d}^e) \le [1-(M-1)\exp(-\gamma_{21})] \cdot [1-(M-1)\exp(-\gamma_{23})] \cdot [1-(M-1)\exp(-\gamma_{3d}^D)] \quad (49)$$

Second, similar assumption can be made for the U_3 cooperation type.

Third, when both U_2 and U_3 provide the correct information from U_1, the SEP of U_1's signals at D is:

$$P_{FC}^e \le (M-1) \cdot Q[\sqrt{2(\gamma_{1d} + \alpha_2 \tilde{\gamma}_{r_2 d} + \alpha_3 \tilde{\gamma}_{r_3 d})}]. \quad (50)$$

Then, we consider the case in which there are detection errors in both U_2 and U_3. It is noticed that the SEP (P_{NC}^e) can be upper bounded by the worst case, which corresponds to the assumption that the partners have decoded the symbol as the farthest constellation point from the actual one sent by U_1 [18]. Based on the worst case, the SEP is:

$$P_{NC}^e \le (M-1) \cdot Q\left[\frac{\sqrt{2}\left(\gamma_{1d} - 2\alpha_2 \tilde{\gamma}_{r_2 d}\beta - 2\alpha_3 \tilde{\gamma}_{r_3 d}\beta\right)}{\sqrt{\gamma_{1d} + 2\alpha_2 \tilde{\gamma}_{r_2 d}\beta + 2\alpha_3 \tilde{\gamma}_{r_3 d}\beta}}\right] \quad (51)$$

where $\beta \coloneqq d^{\max} / d^{\min}$.

The SEPs for the other two cases, in which only one cooperative partner transmits the correct information of U_1, will be expressed as:

$$P_{PC2}^e \le (M-1) \cdot Q\left[\frac{\sqrt{2}\left(\gamma_{1d} + \alpha_2 \tilde{\gamma}_{r_2 d} - 2\alpha_3 \tilde{\gamma}_{r_3 d}\beta\right)}{\sqrt{\gamma_{1d} + \alpha_2 \tilde{\gamma}_{r_2 d} + 2\alpha_3 \tilde{\gamma}_{r_3 d}\beta}}\right] \quad (52)$$

and

$$P_{PC3}^e \le (M-1) \cdot Q\left[\frac{\sqrt{2}\left(\gamma_{1d} - 2\alpha_2 \tilde{\gamma}_{r_2 d}\beta + \alpha_3 \tilde{\gamma}_{r_3 d}\right)}{\sqrt{\gamma_{1d} + 2\alpha_2 \tilde{\gamma}_{r_2 d}\beta + \alpha_3 \tilde{\gamma}_{r_3 d}}}\right]. \quad (53)$$

The corresponding occurrence probabilities for the SEPs in (50)-(53) are:

$$P_1 = P_{r_2} \cdot P_{r_3}, \quad (54)$$

$$P_2 = (1-P_{r_2}) \cdot (1-P_{r_3}), \quad (55)$$

$$P_3 = P_{r_2} \cdot (1-P_{r_3}), \quad (56)$$

$$P_4 = (1-P_{r_2}) \cdot P_{r_3}. \quad (57)$$

By combining (50)-(53) with (54)-(57), the SEP of U_1's signals at D is shown in (58) at the top of the page.

For the convenience of adopting Lemma 2 in [7] to derive the achieved diversity order, it is found that the right-hand side terms of the last inequality in (58) meet the requirements. Lemma 2 of [7] is rewritten below:

***Lemma**: Consider the symbol error probability function P_e satisfying*

$$P_e \le \exp(-\eta_e' \gamma_e) Q[\frac{\sqrt{2}(\eta_c \gamma_c - \eta_e \gamma_e)}{\sqrt{(\eta_c \gamma_c + \eta_e \gamma_e)}}]$$

where $\gamma_c \sim Gamma(n_c, \bar{\gamma})$ *and* $\gamma_e \sim Gamma(n_e, \bar{\gamma})$ *are independent; and* η_c, η_e *and* η'_e *are nonnegative random variables independent of* γ_c *and* γ_e. *If the probability density functions* $p(\eta_c)$, $p(\eta_e)$ *and* $p(\eta'_e)$ *do not depend on* $\bar{\gamma}$, *and* $p(\eta_c \geq 0) = p(\eta_e \geq 0) = p(\eta'_e \geq 0) = 1$, *then the average* P_e *is bounded as* $E[P_e] \leq \kappa \bar{\gamma}^{-(n_c+n_e)}$, *where* $\kappa := E\left[k(\eta_c, \eta_e, \eta'_e)\right] > 0$ *is a constant not dependent on* $\bar{\gamma}$; *hence,* $E[P_e]$ *achieves diversity of order* $n_c + n_e$.

By defining the independent and identically distributed (i.i.d.) random variable $\gamma_{ij}^{norm} \sim Expo(1/\gamma_0) = Gamma(1, \gamma_0)$ for the pair of subscript (i, j), the received SNR of full cooperation is rewritten as:

$$\gamma_{1d} + \alpha_2 \tilde{\gamma}_{r_2 d} + \alpha_3 \tilde{\gamma}_{r_3 d} = \delta_{1d}^2 \gamma_{1d}^{norm} + \alpha_2 \delta_{r_2 d}^2 \gamma_{r_2 d}^{norm} + \alpha_3 \delta_{r_3 d}^2 \gamma_{r_3 d}^{norm} . \quad (59)$$

The first term in the right-hand of inequality (58) is then rewritten as:

$$P_1^e \leq (M-1) \cdot \exp(-\eta'_e \gamma_e) Q\left[\frac{\sqrt{2}(\eta_c \gamma_c - \eta_e \gamma_e)}{\sqrt{(\eta_c \gamma_c + \eta_e \gamma_e)}}\right] \quad (60)$$

where $\gamma_c = \gamma_{1d}^{norm} + \gamma_{r_2 d}^{norm} + \gamma_{r_3 d}^{norm}$, $\gamma_e = 0$, $\eta_c = \min\{\delta_{1d}^2, \delta_{r_2 d}^2 \min(\gamma_{R_2}, \bar{\gamma}_{r_2 d}) / \bar{\gamma}_{r_2 d}, \delta_{r_3 d}^2 \min(\gamma_{R_3}, \bar{\gamma}_{r_3 d}) / \bar{\gamma}_{r_3 d}\}$. As a result, $\gamma_c \sim Gamma(3, \bar{\gamma})$ and $P(\eta_c > 0) = 1$. Application of the lemma above proves that $E[P_1^e]$ achieves diversity of order three.

Similarly, the second term in the right-hand of inequality (58) can be rewritten in the same form as (60) by replacing (M-1) with (M-1)^2. Since the power scale α satisfies $\alpha_i \leq \gamma_{R_i} / \bar{\gamma}_{r_i d}$, the second term meets the requirements with $\gamma_c = \gamma_{1d}^{norm} + \gamma_{r_2 d}^{norm}$, $\gamma_e = \gamma_{R_3}^{norm}$, $\eta_c = \min\{\delta_{1d}^2, \delta_{r_2 d}^2 \min(\gamma_{R_2}, \bar{\gamma}_{r_2 d}) / \bar{\gamma}_{r_2 d}\}$, $\eta_e = 2\beta \delta_{R_3}^2 \tilde{\gamma}_{r_3 d} / \bar{\gamma}_{r_3 d}$, $\eta'_e = \delta_{R_3}^2$. Therefore, $E[P_2^e]$ also achieves diversity of order three.

In the same way, diversity of order three is proved to be achieved by the third term in the right hand of inequality (58).

For the last term, an expression similar to (60) is rewritten by replacing (M-1) with (M-1)^3. In this expression, $\gamma_c = \gamma_{1d}^{norm}$, $\gamma_e = \gamma_{R_2}^{norm} + \gamma_{R_3}^{norm}$, $\eta_c = \delta_{1d}^2$, $\eta_e = \max(2\beta \cdot \delta_{R_2}^2 \tilde{\gamma}_{r_2 d} / \bar{\gamma}_{r_2 d}, 2\beta \cdot \delta_{R_3}^2 \tilde{\gamma}_{r_3 d} / \bar{\gamma}_{r_3 d})$ and $\eta'_e = \min(\delta_{R_2}^2, \delta_{R_3}^2)$. Therefore, $E[P_4^e]$ achieves diversity of order three.

As a result, $E[P_s]$ achieves the diversity of order three, which proves that the proposed hybrid-NCC system can obtain full diversity.

5. Simulation

In this section, we compare the simulated SEP results in various scenarios for practical SNR (γ_0) values. $\gamma_0 = P_x / N_0$ denotes the signal to noise ratio without fading and P_x is the average transmit power. Unless specified otherwise, the adopted modulation is BPSK and the scale of the network is (3, 1).

Fig. 4 shows simulation results of the proposed system under different channel property settings. The average received SNRs of channels *U-U* and channels *U-D* are set to (γ_0 + 10 dB, γ_0), (γ_0, γ_0 + 10 dB) and (γ_0, γ_0) in logarithmic-scale, which correspond to better *U-U* channels, better *U-D* channels and equal average received SNRs between *U-U* and *U-D*, respectively. It demonstrates that when *U-D* channels are better, the system shows lower SEP compared with the other two settings. Additionally, considering that *U-U* channels are better, which is the underlying virtue of the case that users are closed to each other, the transmit power is saved approximately 2 dB at the same SEP compared with the symmetric scenario. As a result, it is suggested that one should choose neighbor users as its partners, based on the pre-received geography information.

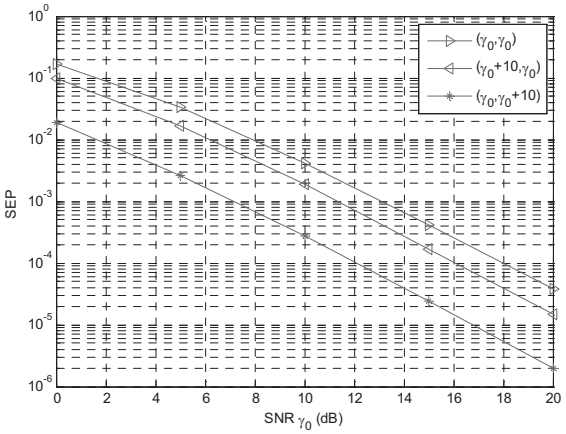

Fig. 4. SEPs of hybrid-NCC in various channel property settings.

For the subsequent simulations, the channel properties are set to (γ_0, γ_0) for comparison simplicity.

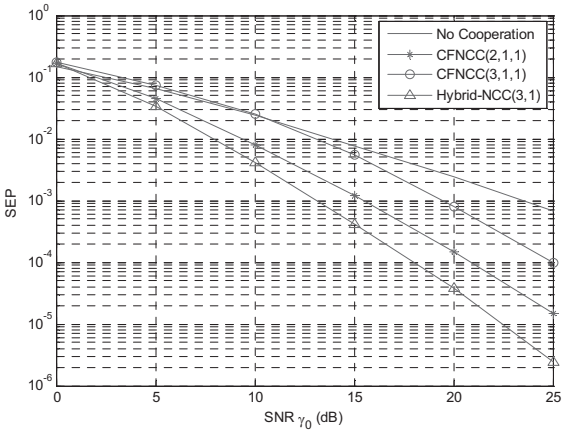

Fig. 5. SEP comparison of hybrid-NCC with CFNC.

Fig. 5 exhibits the SEP comparison of the proposed hybrid-NCC system with the traditional CFNC cooperation [7] at comparable network scale (i.e. three users for the proposed system and two or three users with one relay for

the CFNC cooperation). It is proved that the proposed system achieves more diversity gains and obtains better SEP performance. What's more, dedicated relays are not needed in the proposed system, which reduces the network costs.

The SEP results for the hybrid-NCC system with modulations other than BSPK are shown in Fig. 6. QPSK and 16-QAM are adopted by the proposed system (3, 1) and the CFNC cooperation (2, 1, 1) for comparison. This figure demonstrates that the coding gain of the proposed system decreases when the constellation size is increased, yet it can be improved by optimizing $\boldsymbol{\theta}^T$ as in [19]. Additionally, diversity of order three is achieved by the hybrid-NCC for sufficiently high SNR, while the CFNC cooperation based on the same network size, i.e. two users with one relay, only achieves diversity of order two.

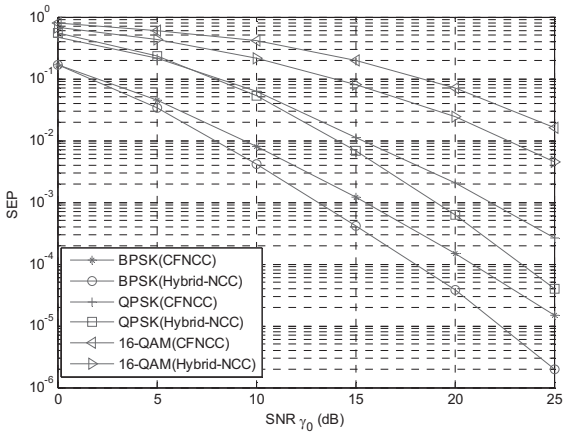

Fig. 6. SEPs of systems with various constellations.

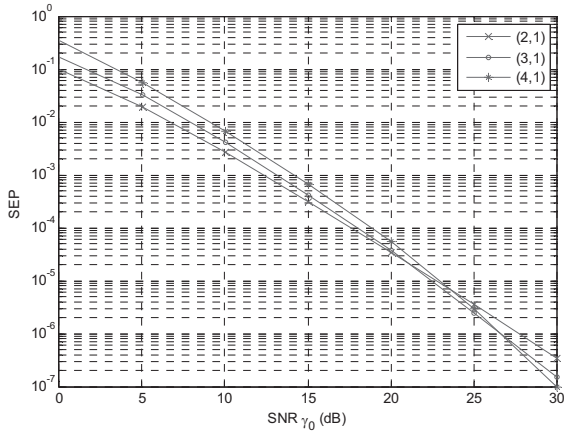

Fig. 7. SEPs of hybrid-NCC with various numbers of cooperative users.

Fig. 7 illustrates SEP results of the proposed system with different numbers of cooperative users. It shows that the diversity gain increases with the number of cooperative users. However, the symbol mapping in the HNCFP implies that there is a coding gain loss at the same time, because the minimum Euclidean distance is decreased. Thus, the number of cooperative users is required to be considered carefully, to balance the coding gains with the diversity gains for different SNR values. Additionally, the demodulator at D becomes more complicated as the number of cooperative users increased.

6. Conclusion

In this paper, a cooperative communication system with the hybrid network coding is proposed. In multiuser networks, users can develop self-organized cooperative sub-networks through partner selection protocol, based on the geographical information. We have analyzed the DMT and the SEP performance of the proposed hybrid-NCC system. The DMT of the hybrid-NCC system is better than that of the existing network coding cooperation. At the same time, by efficiently selecting the LAR parameter α, the system achieves full diversity for the sufficiently high SNR. Additionally, the transmission reliability of the system is improved as compared with that of the traditional CFNCC. Furthermore, dedicated relay nodes are not necessary. In future research, the implementation of the proposed system and the combination of the hybrid-NC and the channel coding (such as LDPC and Turbo) are two aspects to be considered.

Acknowledgements

The authors would like to appreciate the editor and the anonymous reviewers for their thorough review and insightful comments.

References

[1] DING, G., WU, Q., YAO, Y., WANG, J., CHEN, Y. Kernel-based learning for statistical signal processing in cognitive radio networks: Theoretical foundations, example applications, and future directions. *IEEE Signal Processing Magazine*, 2012, vol. 30, no.4, p. 126 - 136.

[2] AHLSWEDE, R., CAI, N., LI, S. Y., YEUNG, R. Network information flow. *IEEE Transactions on Information Theory*, 2000, vol. 46, no. 4, p. 1204 - 1216.

[3] CHEN, Y., KISHORE, S., LI, J. Wireless diversity through network coding. In *Proceedings of IEEE Wireless Communications and Networking Conference*. Las Vegas (USA), 2006, p. 1681 to 1684.

[4] KATTI, S., RAHUL, H., HU, W., KATABI, D., MÉDARD, M., CROWCROFT, J. XORs in the air: practical wireless network coding. *IEEE/ACM Transactions on Networking*, 2008, vol. 16, no. 3, p. 497 - 510.

[5] ZHAN, A., HE, C., JIANG, L. G. Outage behavior in wireless networks with analog network coding. *IEEE Transactions on Vehicular Technology*, 2012, vol. 61, no. 7, p. 3352 - 3360.

[6] PENG, C., ZHANG, Q., ZHAO, M., YAO, Y., JIA, W. On the performance analysis of network-coded cooperation in wireless networks. *IEEE Transactions on Wireless Communications,* 2008, vol. 7, no. 8, p. 3090 - 3097.

[7] WANG, T., GIANNAKIS, G. B. Complex field network coding for multiuser cooperative communications. *IEEE Journal on Selected Areas in Communications*, 2008, vol. 26, no. 3, p. 561 - 571.

[8] LI, G., CANO, A., VILARDEBÓ, J. G., GIANNAKIS, G. B., PÉREZ-NEIRA, A. I. High-throughput multi-source cooperation via complex-field network coding. *IEEE Transactions on Wireless Communications*, 2011, vol. 10, no. 5, p. 1606 - 1617.

[9] WANG, J., LIU, X., CHI, K., ZHAO, X. Complex field network-coded cooperation based on multi-user detection in wireless networks. *Journal of Systems Engineering and Electronics*, 2013, vol. 24, no. 2, p. 215 - 221.

[10] NOSRATINIA, A., HUNTER, T. E. Grouping and partner selection in cooperative wireless networks. *IEEE Journal on Selected Areas in Communications*, 2007, vol. 25, no. 2, p. 369 - 378.

[11] WANG, T., GIANNAKIS, G. B., WANG, R. Smart regenerative relays for link-adaptive cooperative communications. *IEEE Transactions on Communications*, 2008, vol. 56, no. 11, p. 1950 - 1960.

[12] GIANNAKIS, G. B., LIU, Z., MA, X., ZHOU, S. *Space-time Coding for Broadband Wireless Communications*. John Wiley & Sons, Inc., 2007.

[13] ELIA, P., KUMAR, K. R., PAWAR, S. A., KUMAR, P. V., LU, H. F. Explicit space-time codes achieving the diversity-multiplexing gain tradeoff. *IEEE Transactions on Information Theory*, 2006, vol. 52, no. 9, p. 3869 - 3884.

[14] ZHENG, L., TSE, D. N. C. Diversity and multiplexing: A fundamental tradeoff in multiple antenna channels. *IEEE Transactions on Information Theory*, 2003, vol. 49, no. 5, p. 1073 - 1096.

[15] ZOU, Y., YAO, Y. D., ZHENG, B. Opportunistic distributed space-time coding for decode-and-forward cooperation systems. *IEEE Transactions on Signal Processing*, 2012, vol. 60, no. 4, p. 1766 - 1781.

[16] LANEMAN, J., WORNELL, G. Distributed space-time-coded protocols for exploiting cooperative diversity in wireless networks. *IEEE Transactions on Information Theory*, 2003, vol. 49, no. 10, p. 2415 - 2425.

[17] BLETSAS, A., KHISTI, A., REED, D., LIPPMAN, A. A simple cooperative diversity method based on network path selection. *IEEE Journal on Selected Areas in Communications*, 2006, vol. 24, no. 3, p. 659 - 672.

[18] WANG, T., CANO, A., GIANNAKIS, G. B., LANEMAN, J. N. High-performance cooperative demodulation with decode-and-forward relays. *IEEE Transactions on Communications*, 2007, vol. 55, no. 7, p. 1427 - 1438.

[19] XIN, Y., WANG, Z., GIANNAKIS, G. B. Space-time diversity systems based on linear constellation precoding. *IEEE Transactions on Wireless Communications*, 2003, vol. 2, no. 2, p. 294 to 309.

About Authors ...

Gengrun WANG was born in Anhui, China, on November 15, 1987. He received his B.S. degree in Information Engineering in 2009 from Zhejiang University (ZJU), Hangzhou, China. He is currently working towards the Ph.D. degree in satellite communication in PLA University of Science and Technology (PLAUST). His research interests include performance analysis of cooperative networks and OFDM based techniques in satellite communication.

Daoxing GUO was born in 1974. He received his Ph.D. degree from the Institute of Communication Engineering in 2002. He is currently a professor at PLA University of Science and Technology. His research interests include satellite communications, cooperative networks and signal processing in communications.

Aijun LIU was born in 1970. He received his Ph.D. degree from the Institute of Communication Engineering in 1996. He is currently a professor at PLA University of Science and Technology. His primary research work and interests are in the area of wireless communication and signal process.

Bangning ZHANG was born in Anhui Province, China, in 1963. He received the M.S. degree in 1987. He is now a professor and Ph.D. supervisor. His research interests include satellite communications and signal processing in communications.